Nuclear medium effects in pion elastic scattering and charge exchange

W. B. Kaufmann
Department of Physics, Arizona State University, Tempe, Arizona 85281

W. R. Gibbs
Theoretical Division, Los Alamos National Laboratory, Los Alamos, New Mexico 87545
and Department of Physics, Arizona State University, Tempe, Arizona 85281

(Received 21 March 1983)

The three body approximation of the pion-nucleus optical model is used to calculate effective strengths to be used in conventional calculations. The resulting wave functions are used to calculate pion elastic scattering and single charge exchange. It is found that observed energy shifts in elastic scattering can be understood. Considerable change in the magnitude and shape (as a function of energy) of the charge exchange cross section is a direct result of these corrections.

[NUCLEAR REACTIONS $^{12}C(\pi^+,\pi^+)^{12}C$, $^{7}Li(\pi^+,\pi^0)^{7}Be$, $^{13}C(\pi^+,\pi^0)^{13}N$, $^{15}N(\pi^+,\pi^0)^{15}O$; calculated $d\sigma/d\Omega(0°)$, $\sigma(\theta)$, $\sigma(E)$; corrections due to binding and Pauli blocking.]

I. INTRODUCTION

A fundamental ingredient in the calculation of pion-nucleus interactions is τ, the scattering amplitude of the pion on a bound nucleon. Since τ involves coordinates of all the nucleons in the nucleus it is a many-body operator and is notoriously difficult to compute. If the energy of the pion is much greater than E_b, the binding energy of the nucleon, and if the pion-nucleon t matrix (t) is insensitive to energy variations over the range $E \pm E_b$, then τ can be replaced by t, the free pion-nucleon t matrix (impulse approximation). Since t is a two-body operator the practical simplification is enormous. Unfortunately, these conditions certainly fail to apply at the energies most commonly used at the meson factories. Nonetheless, due to its seductive simplicity many workers in the field have continued to use the impulse approximation in this regime.

To make up for the theoretical deficiencies of this potential a common procedure is to replace τ by a general form with parameters chosen through use of pion-nuclear data. A particularly interesting phenomenological calculation was performed by Cottingame and Holtkamp[1] who find that the appropriate t matrix is approximately the free one evaluated at a lowered energy,

$$t_{\text{phenom}}(E) = t_{\text{free}}(E - D) .$$

For a pion with laboratory kinetic energy between 100 and 300 MeV, D is found to be around 30 MeV with generous error bars. Cottingame and Holtkamp make the eminently plausible suggestion that the energy shift is due to nucleon binding effects.

The idea of introducing an energy shift in the free pion-nucleus t matrix to represent binding effects was introduced by Schmit in 1972.[2] He attempted to make estimates of the size of this shift, but in models available at that time even the sign was uncertain. The calculation of the energy shift is improved through the introduction of a three-body model in which τ is obtained (in principle) from the solution of three-body equations in which the pion interacts with one nucleon and this one nucleon interacts with a central core.[3–5] As the reactive content of the optical model became better understood[6] applications of truncated forms of the three-body model were made.[7–9]

Recently, calculations have been performed in which the interaction of the intermediate nucleon is kept, one for pion scattering on ^{16}O with a nonrealistic pion-nucleon t matrix[10] and one for pion scattering on ^{12}C with a realistic pion-nucleon t matrix.[11] These calculations have the advantage of including effects left out of previous work (e.g., a realistic intermediate potential, Saxon-Woods including Coulomb) but they have the disadvantage that no simple physical parameters are visible, such as the energy shift. They also, at present, must be tailored to a given nucleus which makes general understanding of the effects as a function of nuclear mass very difficult. For the calculation of reactions, distorted waves are needed for distorted-wave impulse approximation (DWIA) matrix elements, and these models are too complex, at present, to yield these wave functions on demand.

In this paper we treat a model which is intermediate in the sense that the core interaction is taken into account but has a discrete spectrum and can be calculated for any (closed-shell) nucleus. In calculating pion charge exchange it has been noted that Pauli blocking effects are important. These blocking effects were included in elastic scattering by Landau and Thomas[8] and by Landau and McMillan.[12] They were also included in the calculation of charge exchange by Landau and Thomas.[13] These authors used a nuclear matter approach whose validity (especially on light nuclei and for surface peaked reactions) is not clear.

In the fixed scatterer approximation it was possible to introduce Slater determinants and provide a partial in-

clusion of the effects of fermion antisymmetry.[14,15] Although these models are rather different, the size of the blocking effects is similar. The Appendix of this paper presents a discussion of the relation of Pauli blocking to classical notions.

Section II develops the necessary formalism for the general case starting from the work of Ref. 11. In Sec. III the approximate reduction of the multiterm separable potential derived in Sec. II to the more standard nonlocal form is made. Both on-shell and off-shell corrections are considered, the former being discussed in terms of energy shifts and Pauli blocking and the latter in terms of intermediate state (mostly delta) propagation. This section is done with the intermediate state being described by the spectrum (and wave functions) of an infinite square well and for isoscalar nuclei. Section IV relaxes these two assumptions by considering a harmonic oscillator intermediate state and both isoscalar and isovector parts to the optical potential. Also discussed are improvements to the Pauli blocking expressions. Section V gives the results of DWIA calculations using distorted waves calculated with methods of Sec. III. Noticeable changes in shape and magnitude (over traditional DWIA calculations) occur. Section VI discusses the shortcomings of the present calculation and suggests improvements.

II. FORMALISM

The t matrix (τ) describing the interaction of the pion with the jth nucleon satisfies the equation

$$\begin{aligned}\tau &= V_{\pi N} + V_{\pi N} G V_{\pi N} \\ &= V_{\pi N} + V_{\pi N} G_0 \tau ,\end{aligned} \tag{1}$$

where

$$G_0 = (\mathscr{E} - H_0 + i\epsilon)^{-1}, \quad H_0 = T_c + T_N + T_\pi + V_{jc} ,$$
$$G = (\mathscr{E} - H + i\epsilon)^{-1}, \quad H = T_c + T_N + T_\pi + V_{jc} + V_{\pi N} ,$$

and T_c, T_N, and T_π are the core, struck nucleon, and pion kinetic energies. H_0 includes the nucleon-core interaction V_{jc}, but not the pion-nucleon interaction $V_{\pi N}$.

Note that it is the operator τ which is used to generate the optical potential, hence the properties of τ (not t, the free pion nucleon t matrix) determine the rate of convergence of the series for the optical potential. If τ has a large nonlocality then higher order terms will be small, both for the quasielastic (Lorentz-Lorenz) parts[16] and the true absorption parts,[17] regardless of the behavior of the actual pion-nucleon t matrix.

Following Ref. 11 we make an approximate decomposition of the Hamiltonian,

$$H \cong H_{\pi N}(\vec{p},\vec{r}) + H_{jc}(\vec{P},\vec{R}) , \tag{2}$$

where

$$\begin{aligned}H_{\pi N}(\vec{p},\vec{r}) &= \frac{p^2}{2\mu_{\pi N}} + V_{\pi N}(\vec{r}) , \\ \mu_{\pi N} &= M_\pi M_N/(M_\pi + M_N) ,\end{aligned} \tag{3}$$

and we have used the approximation

$$V_{jc}(\vec{r}_j - \vec{r}_c) \cong V_{jc}(\vec{R}) . \tag{4}$$

Here $\vec{p}$ and $\vec{r}$ refer to the relative coordinates in the π-N system and $\vec{P},\vec{R}$ refer to the center of mass coordinate of the π-N system relative to the core. The approximation in Eq. (4) is a good one if $V_{\pi N}$ is short-ranged relative to V_{jc}, i.e., if the pion-nucleon interaction is short-ranged compared to the nucleon-nucleus interaction. The small mass of the pion improves this approximation as well.[11]

With this approximation

$$\begin{aligned}H_{jc}(\vec{P},\vec{R}) &\cong \frac{P^2}{2\mu_{\pi N,c}} + V_{jc}(\vec{R}) , \\ \mu_{\pi N,c} &= (M_\pi + M_N)M_c/(M_\pi + M_N + M_c) ,\end{aligned} \tag{5}$$

and the spectrum separates into a product space

$$H_{\pi N} \mid \chi_\nu \rangle = \mathscr{E}_\nu \mid \chi_\nu \rangle , \tag{6}$$

$$H_{jc} \mid \Phi_A \rangle = E_A \mid \Phi_A \rangle . \tag{7}$$

The nuclear single-particle states are eigenstates of

$$H'_{jc}(\vec{q},\vec{\rho}) = \frac{q^2}{2\mu_{jc}} + V_{jc}(\vec{\rho}) , \tag{8}$$

where $\vec{\rho} = \vec{r}_j - \vec{r}_c$ is the nucleon-core separation and $\vec{q}$ is the relative nucleon-core momentum. The functional forms of H_{jc} and H'_{jc} are nearly the same ($\mu_{\pi N,c} \cong \mu_{jc}$ to about 15%) so they have nearly the same spectrum. We make the approximation that the spectra (and eigenstates) of these systems are equivalent. Taking matrix elements of Eq. (1) with respect to the eigenstates of Eqs. (6) and (7), we are led to [see Ref. 11, Eqs. (21) and (23)]

$$\langle \vec{k}' \mid V_{\rm opt}(E) \mid \vec{k} \rangle = \sum_A \int d\vec{q}\,' d\vec{q} \phi^*_A(\vec{q}\,') \left[\sum_{A'} \phi_{A'}(\vec{P}') \langle \vec{p}\,' \mid V_{\pi j} \mid \vec{p} \rangle \phi^*_{A'}(\vec{P}) + \sum_{A'} \phi_{A'}(\vec{P}') \sum_\nu \frac{\langle \vec{p}\,' \mid V_{\pi j} \mid \chi_\nu \rangle \langle \chi_\nu \mid V_{\pi j} \mid \vec{p} \rangle}{E + E_A - \mathscr{E}_\nu - E_{A'} + i\epsilon} \phi^*_{A'}(\vec{P}) \right] \phi_A(\vec{q}) , \tag{9}$$

where

$$\vec{p}=-a\vec{q}+b\vec{k},\quad \vec{P}=\vec{q}+c\vec{k}$$

and

$$a=\frac{m_\pi}{m_j+m_\pi}\quad(\cong 0)\,,$$
$$b=\frac{m_j(m_\pi+m_j+m_c)}{(m_j+m_\pi)(m_j+m_c)}\quad(\cong 1)\,, \tag{10}$$
$$c=\frac{m_c}{m_j+m_c}\quad(\cong 1)\,,$$

and $\vec{k}$ is the pion momentum in the three-body c.m.

The Watson restriction to include only excited intermediate states in the Green's function part of Eq. (9) can be enforced, at least approximately, by confining A' to nonfilled levels. Note that A labels occupied orbitals in the target nucleus so that A' is summed over a complementary set to A in the second term. We will generally refer to this as a Pauli blocking requirement, although the procedure is just the approximate calculation of the Watson optical model. The sum over A' in the first term of Eq. (9) arises from closure and hence includes the entire spectrum.[11]

Considering the A' sum in two parts, i.e., one sum over the set of occupied states $A'\in O$ and another over unoccupied states $A'\in\sim O$, and recognizing that the free t matrix is given by [Eq. (26), Ref. 11]

$$\langle\vec{p}\,'|t_{\pi N}(E)|\vec{p}\rangle=\langle\vec{p}\,'|V_{\pi N}|\vec{p}\rangle+\sum_\nu\frac{\langle\vec{p}\,'|V_{\pi N}|\chi_\nu\rangle\langle\chi_\nu|V_{\pi N}|\vec{p}\rangle}{E-\mathfrak{E}_\nu+i\epsilon}\,, \tag{11}$$

we may write

$$\langle\vec{k}\,'|V_{\rm opt}(E)|\vec{k}\rangle=\sum_A\int d\vec{q}\,d\vec{q}\,'\phi_A^*(\vec{q}\,')\sum_{A'}[\phi_{A'}(\vec{P}\,')\langle\vec{p}\,'|\theta^{AA'}|\vec{p}\rangle\phi_{A'}^*(\vec{P})]\phi_A(\vec{q})\,, \tag{12}$$

where

$$\langle\vec{p}\,'|\theta^{AA'}|\vec{p}\rangle=\begin{cases}\langle\vec{p}\,'|V_{\pi N}|\vec{p}\rangle & \text{if } A'\in O\\ \langle\vec{p}\,'|t_{\pi N}(E+E_A-E_{A'})|\vec{p}\rangle & \text{if } A'\in\sim O\,.\end{cases} \tag{13}$$

At low incident pion energy the "blocked" terms have strongest weighting and considerable mixing of V may occur, but at high energies the "t" pieces will dominate and the energy shifted sum of the t matrix produces the optical potential. Note that in principle, the t matrix must be known to all energies down to $-\infty$. In practice our results are not sensitive to this region, hence for $E<0$ we have used the threshold amplitudes. This process is presumably the cause of the energy shift and Pauli blocking effects. We neglect recoil effects taking the (rather extreme) approximations $a=0$, $b=1$, and $c=1$, so that the equations simplify:

$$\vec{p}=\vec{k},\quad \vec{P}=\vec{q}+\vec{k}\,, \tag{14}$$
$$\langle\vec{k}\,'|V_{\rm opt}(E)|\vec{k}\rangle=\sum_{A\in O}\sum_{A'}\langle\vec{k}\,'|\theta^{AA'}|\vec{k}\rangle\int d\vec{q}\,d\vec{q}\,'\phi_A^*(\vec{q}\,')\phi_{A'}(\vec{q}\,'+\vec{k}\,')\phi_A(\vec{q})\phi_{A'}^*(\vec{q}+\vec{k})\,.$$

For orientation, note that if we neglect Pauli blocking and the energy dependence of the t matrix then

$$\begin{aligned}\langle\vec{k}\,'|V_{\rm opt}(E)|\vec{k}\rangle&=\langle\vec{k}\,'|t(E)|\vec{k}\rangle\sum_{A\in O}\int d\vec{q}\,d\vec{q}\,'\phi_A^*(\vec{q}\,')\phi_A(\vec{q})\sum_{A'}\phi_{A'}^*(\vec{q}\,'+\vec{k}\,')\phi_{A'}(\vec{q}+\vec{k})\\&=\langle\vec{k}\,'|t(E)|\vec{k}\rangle\sum_{A\in O}\int d\vec{q}\,d\vec{q}\,'\phi_A^*(\vec{q}\,')\phi_A(\vec{q})\delta(\vec{q}\,'+\vec{k}\,'-\vec{q}-\vec{k})\\&=\langle\vec{k}\,'|t(E)|\vec{k}\rangle\sum_{A\in O}\int d\vec{q}\,\phi_A^*(\vec{q}+\vec{k}-\vec{k}\,')\phi_A(\vec{q})\\&=\langle\vec{k}\,'|t(E)|\vec{k}\rangle\rho(\vec{k}-\vec{k}\,')\end{aligned} \tag{15}$$

and the "t-ρ" approximation is recovered.

If either the energy dependence of the t matrix is important or the energy is low enough for the Pauli effects to be important the t-ρ approximation will be poor. Note that if all intermediate states are kept (no Pauli) and the energy dependence of t is neglected (as above) then whether the eigenfunctions of Eq. (5) or (8) are used is immaterial since both are complete. This means that the error introduced by our approximations is only in the *correction* to closure and not in the total potential.

We may write Eq. (14) as

$$\langle\vec{k}\,'|V_{\rm opt}(E)|\vec{k}\rangle=\sum_{A\in O}\sum_{A'}\langle\vec{k}\,'|\theta^{AA'}|\vec{k}\rangle\times I_{AA'}(\vec{k})I_{AA'}^*(\vec{k}\,')\,, \tag{16}$$

where

$$I_{AA'}(\vec{k})=\int d\vec{q}\,\phi^*_{A'}(\vec{q}+\vec{k})\phi_A(\vec{q})\ . \tag{17}$$

Assuming that the pion-nucleon t matrix is separable [see Eq. (33)], Eq. (14) represents a multiterm separable pion-nucleus potential. The explicit form of this potential is developed below.

Since

$$\phi_A(\vec{q})=(2\pi)^{-3/2}\int d\vec{r}\,e^{-i\vec{q}\cdot\vec{r}}\phi_A(\vec{r})$$

we have

$$I_{AA'}(\vec{k})=\int d\vec{r}\,\phi^*_{A'}(\vec{r})\phi_A(\vec{r})e^{i\vec{k}\cdot\vec{r}}\ . \tag{18}$$

Using nuclear wave functions of the form

$$\phi_A(\vec{r})=\phi_{nl}(r)Y_{lm}(\vec{r})\equiv\phi_\alpha(r)Y_{lm}(\hat{r}) \tag{19}$$

and expanding the exponential in spherical harmonics, we obtain

$$I_{AA'}(\vec{k})=4\pi\sum_{\lambda\mu}i^\lambda I^\lambda_{\alpha\alpha'}(k)\left[\frac{(2\lambda+1)(2l'+1)}{4\pi(2l+1)}\right]^{1/2}\times\begin{bmatrix}l' & \lambda & | & l\\ m' & \mu & | & m\end{bmatrix}\begin{bmatrix}l' & \lambda & | & l\\ 0 & 0 & | & 0\end{bmatrix}Y_{\lambda\mu}(\hat{k})\ , \tag{20}$$

where

$$I^\lambda_{\alpha\alpha'}(k)=\int_0^\infty r^2dr\,\phi_\alpha(r)\phi_{\alpha'}(r)j_\lambda(kr) \tag{21}$$

and the expressions in the brackets represent Clebsch-Gordan coefficients. The optical potential now becomes

$$\langle\vec{k}'\,|\,V_{\rm opt}(E)\,|\,\vec{k}\rangle=\sum_{\lambda\alpha\alpha'}(2l+1)(2l'+1)I^\lambda_{\alpha\alpha'}(k)I^\lambda_{\alpha\alpha'}(k')\begin{bmatrix}l & l' & | & \lambda\\ 0 & 0 & | & 0\end{bmatrix}^2\langle\vec{k}'\,|\,\theta^{\alpha\alpha'}\,|\,\vec{k}\rangle P_\lambda(x)\ , \tag{22}$$

where $x=\hat{k}\cdot\hat{k}'$.

Finally we decompose the (spin averaged) πN t matrix into partial waves,

$$\langle\vec{k}'\,|\,\theta^{\alpha\alpha'}\,|\,\vec{k}\rangle=\sum_L\theta^{\alpha\alpha'}_L(E,k,k')P_L(x)\ , \tag{23}$$

to obtain

$$\langle\vec{k}'\,|\,V_{\rm opt}(E)\,|\,\vec{k}\rangle=\sum_{l_\pi}V_{l_\pi}(k,k')P_{l_\pi}(x)\ , \tag{24}$$

where

$$V_{l_\pi}(E,k,k')=\sum_L\sum_{\alpha\alpha'}H^{l_\pi}_{\alpha\alpha' L}(k,k')\theta^{\alpha\alpha'}_L(E,k,k') \tag{25}$$

and

$$H^{l_\pi}_{\alpha\alpha' L}(k,k')=\sum_\lambda(2l+1)(2l'+1)\begin{bmatrix}l & l' & | & \lambda\\ 0 & 0 & | & 0\end{bmatrix}^2\begin{bmatrix}\lambda & L & | & l_\pi\\ 0 & 0 & | & 0\end{bmatrix}^2 I^\lambda_{\alpha\alpha'}(k)I^\lambda_{\alpha\alpha'}(k')\ . \tag{26}$$

In Eq. (25) α is summed over occupied levels and α' over all levels. Equations (22)–(26), which incorporate binding effects and Pauli blocking in the pion nucleus optical potential, are the principal results of the work to this point and constitute the basis for the remainder of the paper.

At pion energies of less than 400 MeV, t and v are well described with $L=0$ and 1; thus we need only

$$H^{l_\pi}_{\alpha\alpha' 0}(k,k')=(2l+1)(2l'+1)\begin{bmatrix}l & l' & | & l_\pi\\ 0 & 0 & | & 0\end{bmatrix}^2 I^{l_\pi}_{\alpha\alpha'}(k)I^{l_\pi}_{\alpha\alpha'}(k') \tag{27}$$

and

$$H^{l_\pi}_{\alpha\alpha' 1}(k,k')=\frac{l_\pi}{2l_\pi-1}H^{l_\pi-1}_{\alpha\alpha' 0}(k,k')+\frac{l_\pi+1}{2l_\pi+3}H^{l_\pi+1}_{\alpha\alpha' 0}(k,k')\ .$$

Equation (25) suggests a natural definition of the average over α and α',

$$\sum_{\alpha\alpha'}H^{l_\pi}_{\alpha\alpha' L}(k,k')\theta^{\alpha\alpha'}_L(E,k,k')\equiv\sum_{\alpha\alpha'}H^{l_\pi}_{\alpha\alpha' L}(k,k')\tilde{\theta}^{l_\pi}_L(E,k,k')$$
$$\equiv H^{l_\pi}_L(k,k')\tilde{\theta}^{l_\pi}_L(E,k,k')\ . \tag{28}$$

Note that $H^{l_\pi}_0(k,k')$ is just the closure result, i.e., the l_π projection of the density

$$H^{l_\pi}_0(k,k')=\int r^2dr\,j_{l_\pi}(kr)\rho(r)j_{l_\pi}(k'r)\ . \tag{29}$$

Equation (28) may also be used to define an average energy by

$$\tilde{E}_L^{l_\pi}=\sum_{\alpha\alpha'}\frac{H^{l_\pi}_{\alpha\alpha' L}(k,k')(E+E_\alpha-E_{\alpha'})}{H_L^{l_\pi}(k,k')}\ , \tag{30}$$

where $k=k'=k_0$ and k_0 is the on-shell momentum.

For a t matrix which is not too rapidly varying with energy, this is the effective energy to be used in the evaluation of t. To see this, expand the on-shell t matrix $t_L(E)$ about $\tilde{E}_L^{l_\pi}$,

$$t_L(E+E_\alpha-E_{\alpha'})$$

$$\cong t_L(\tilde{E}_L^{l_\pi})+\left.\frac{dt_L}{dE}\right|_{\tilde{E}_L^{l_\pi}}(E+E_\alpha-E_{\alpha'}-\tilde{E}_L^{l_\pi})\ , \tag{31}$$

so that, upon averaging

$$\tilde{t}_L(E)\cong t_L(\tilde{E}_L^{l_\pi}) \tag{32}$$

where Eqs. (28) and (30) have been used. Note that the effective energy is a function of L and l_π. The more general off-shell case is discussed in the next section.

III. REDUCTION TO STANDARD FORM

One could carry out the solution of the equations given in the last section and indeed this is a useful pursuit. In fact, it has been done for the two nuclei ^{12}C (Ref. 11) and ^{16}O (Ref. 10) for the difficult case in which intermediate continuum nuclear states are treated. In this section, however, we wish to calculate the effects on the more common forms of the (finite or zero range) pion nucleus optical potential. The reason for this is twofold. First, the corrections can then be inserted into any optical model code (coordinate or momentum space) so that distorted waves for reactions can be calculated. Second, this reduction gives physical insight into the nature of the corrections, the physical effects included, and the errors due to neglected higher order terms.

We take the form of the πN t matrix to be

$$t(E,\vec{k},\vec{k}')\sim b_0(E)v_0(k)v_0(k')+b_1(E)v_1(k)v_1(k')\vec{k}\cdot\vec{k}'\ , \tag{33}$$

where the strengths $b_L(E)$ depend only on the πN center-of-mass energy and may be evaluated in terms of πN phase shifts. For this form the pion-nucleon momentum dependence (v_0 or v_1) factors out of the energy sum in Eq. (25) and the standard form of the optical potential is recovered except that the b's are replaced by

$$\tilde{b}_L^{l_\pi}(E,k,k')=\sum_{\alpha\alpha'}\frac{H^{l_\pi}_{\alpha\alpha' L}(k,k')b_L(E+E_\alpha-E_{\alpha'})}{H_L^{l_\pi}(k,k')}\ . \tag{34}$$

The effective strengths have gained two dependences that they did not have before. These are a dependence on the pion-nucleus partial wave (l_π) and a dependence on the off-shell momenta (k,k'). The l_π causes no problems since optical model codes solve each pion-nucleus partial wave separately and a different strength can easily be inserted for each value of l_π. The k,k' dependence is more of a problem since b_L is solely a function of energy in the standard optical codes. Later in this section we will discuss an approximate way to incorporate this off-shell dependence. For the present we consider only the on-shell values of $\tilde{b}_L^{l_\pi}$.

In this section the functions ϕ_{nl}, introduced in Eq. (19), will be taken to be solutions in a spherical box

$$\phi_{nl}(r)=j_l(k_{nl}r)\quad r<R$$
$$=0\quad r\geq R\ ,$$

where k_{nl} is defined by $j_l(k_{nl}R)=0$.

This model crudely reproduces the true single particle spectrum and is similar to the harmonic oscillator spectrum considered in Sec. IV.

Note that for this case there is no difference between the eigenfunctions of Eqs. (5) and (8) so that the Pauli blocking does not require an additional approximation. The energies in the θ matrix are taken from Eq. (5) using a relativistic generalization of $\mu_{\pi N,c}$, i.e., by replacing the masses by total energies. We consider here only the isoscalar case. The generalization to the isovector case is deferred until Sec. IV.

As indicated in Eq. (13) the effect of blocking is to replace the t matrix of a filled level by the corresponding potential; hence the potentials describing each individual partial wave in the pion-nucleon system must be known. There is indeed a large variety of such potentials in the literature and the results of our work will depend upon the details of these functions. Since the potentials are real below the pion production threshold, the imaginary part of θ is zero for the blocked terms. In this section we make the additional approximation that the *real part* of θ (i.e., the potential) is also zero for the blocked levels. In Sec. IV we discuss the effect of using the potential for the s waves; we find a substantial correction only at low energies.

The effective strengths for a leadlike nucleus are shown in Fig. 1. The plots are given as a function of l/k so comparison with nuclear size can be made. For this large nucleus the Pauli effect is nearly a constant multiplier for partial waves corresponding to impact parameters smaller than the nuclear radius. Thus the use of a single reduction factor, such as one from a nuclear matter description, is not unreasonable.

Figure 2 shows the p-wave effective strengths for ^{16}O. Here the effect of the finite size of the nucleus is clear as the blocking effect becomes smaller at the surface. Note that the larger reduction of b_1 with increasing density can mock up the nonlinear ρ dependence of the Lorentz-Lorenz effect and would be difficult to distinguish from L-L behavior if the geometry of the scattering were examined empirically.[18]

For elastic scattering (at least near the 3-3 resonance) the surface partial waves are the most important and are approximately the same as the $l_\pi=0$ unblocked wave. In Fig. 3 the real and imaginary parts of b_1 are compared with the results of Ref. 1. For the large component ($\mathrm{Im}b_1$), the agreement is excellent.

Consider the half-off-shell amplitude defined by Eq. (34),

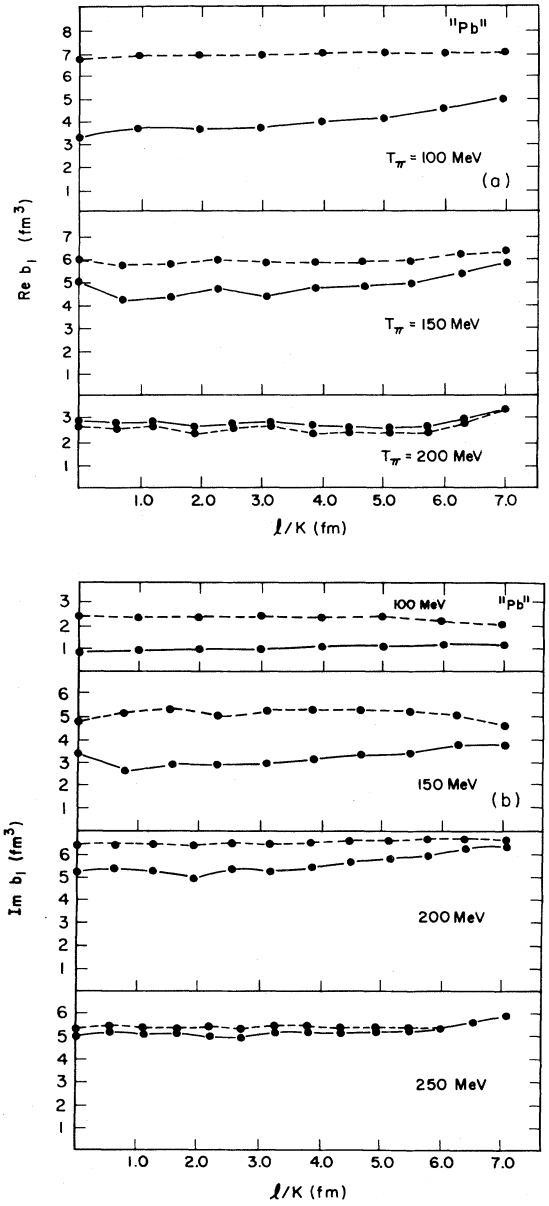

FIG. 1. Effective strengths for a heavy nucleus. Both the real (a) and imaginary (b) parts of the p-wave strength are shown. The dotted curve is the result of including the t matrix (energy shifted) in all terms of the sum in Eq. (25). The solid curve is the result of replacing the t matrix by zero for the occupied states.

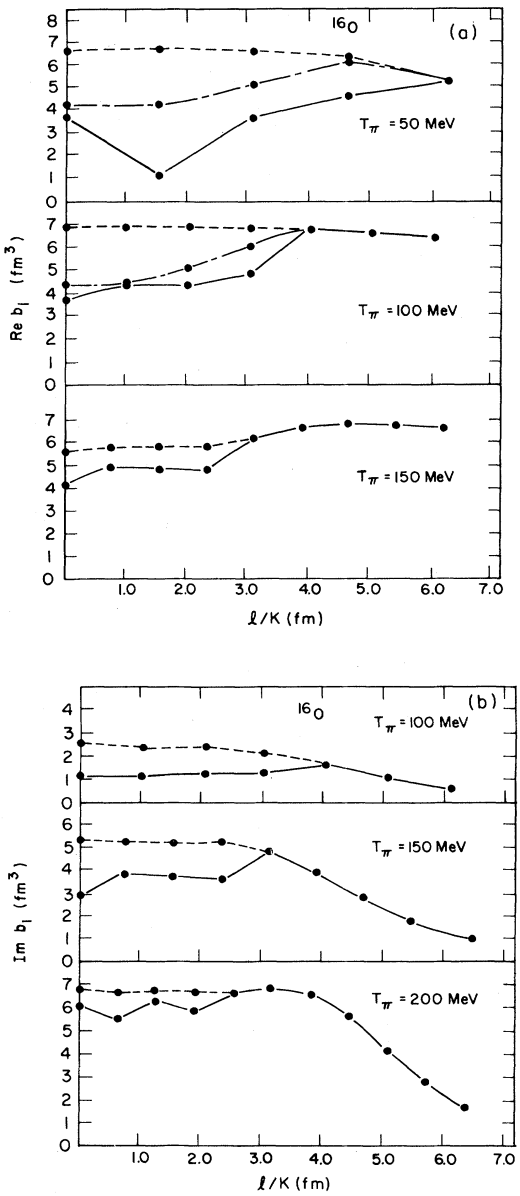

FIG. 2. Effective strengths for a light nucleus. For the meaning of the dashed and solid curves see the caption of Fig. 1. The dashed-dotted curve is an estimate of what might be expected from an effective Lorentz-Lorenz effect.

$$\tilde{b}_1^{l_\pi}(E,k_0,k)=\frac{\sum_{\alpha\alpha'} H^{l_\pi}_{\alpha\alpha' 1}(k_0,k) b_1(E+E_\alpha-E_{\alpha'})}{H_1^{l_\pi}(k_0,k)}=b_1(\tilde{E}_1^{l_\pi})+\frac{d}{dE}b_1(E)\Big|_{\tilde{E}_1^{l_\pi}}\frac{\sum_{\alpha\alpha'} H^{l_\pi}_{\alpha\alpha' 1}(k_0,k)(E+E_\alpha-\tilde{E}_{\alpha'}-\tilde{E}_1^{l_\pi})}{H_1^{l_\pi}(k_0,k)}+\cdots . \tag{35}$$

Note that the term with lowest order dependence on k is proportional to the derivative of $b_1(E)$ which is proportional to the derivative of the amplitude which is, in turn, proportional to the lifetime of the intermediate state.[17] The additional off-shell behavior is equivalent to a change in the nonlocality of the pion-nucleon amplitude. This is physically due to

the propagation of the intermediate state in that an additional size of the pion-nucleon system is associated with its motion during the interaction time. This effect is well known in delta-hole models[19] and is thought of as "delta propagation." It has been pointed out previously that such considerations lead to an additional effective nonlocality in the interaction.[20]

If we wish to use "standard" (i.e., Kisslinger or finite-range-separable) optical model codes we are at an impasse since the strength parameters b_L in such codes are momentum independent. As a first step we rearrange Eq. (34) to get

$$\tilde{b}_L^{l\pi}(E)\left[\frac{\tilde{b}_L^{l\pi}(E,k,k')}{\tilde{b}_L^{l\pi}(E,k_0,k_0)}\right]H_L^{l\pi}(k,k')\equiv\tilde{b}_L^{l\pi}(E)W_L^{l\pi}(E,k,k')H_L^{l\pi}(k,k')\ , \tag{36}$$

where

$$\tilde{b}_L^{l\pi}(E)\equiv\tilde{b}_L^{l\pi}(E,k_0,k_0)$$

and k_0 is the on-shell momentum, which corresponds to energy E. The off-shell behavior induced by the sum over the energy spectrum (α,α') has now been concentrated into a correction factor W_L which is unity on the energy shell.

To proceed further we assume that the major effect of $W_L(E,k,k')$ is to modify the *range* of the off-shell form factors (v_L) of the πN t matrix [Eq. (33)]. This is clearly an approximation as the k,k' dependence of W does not factor. To estimate the range we study the half-off-shell potential, which consists of terms of the form

$$\tilde{b}_L^{l\pi}(E)W_L^{l\pi}(k_0,k)H_L^{l\pi}(k_0,k)\ .$$

Table I gives values of $W_L^{l\pi}(k_0,k)$ for $k=k_0+1$ (fm^{-1}). The general form of W_L can be seen from Fig. 4 which compares $H_L^{l\pi}(k_0,k)$ with the modified nuclear density

$$\tilde{H}_L^{l\pi}(k_0,k)\equiv W_L^{l\pi}(k_0,k)H_L^{l\pi}(k_0,k)\ .$$

$W_L^{l\pi}(k_0,k)$ is further simplified if T_π is below 200 MeV, being approximately expressible as

$$W_1^{l\pi}(k_0,k)\cong\frac{k_0^2+\Lambda_{l\pi}^2}{k^2+\Lambda_{l\pi}^2}\ , \tag{37}$$

where Λ_{π_l} is an empirical range parameter whose values are given in Table I.

For comparison, the distance of travel of the delta during its lifetime ($\sim$0.35 fm) corresponds to a range in momentum space of $\sim$560 MeV/c. The addition of this nonlocality to the natural nonlocality of the pion-nucleon t matrix in the 33 channel (now thought to be around 500–600 MeV/c by comparison with the πNN vertex[21] makes the effective off-shell momentum range rather small ($\sim$300–400 MeV/c). This, in turn, makes the higher order optical potential less important.[16] In other words, the combination of the size of the pion-nucleon system and the motion of the delta decreases the importance (observability) of nucleon-nucleon correlations.

In this paper we have used the correct values of $b_L^\pi(E)$ as computed from Eq. (34) with $k=k'=k_0$. Instead of the off-shell factor $W_L^{l\pi}$ we have adjusted the off-shell range of the π-N t matrix to 300 MeV/c as just discussed.

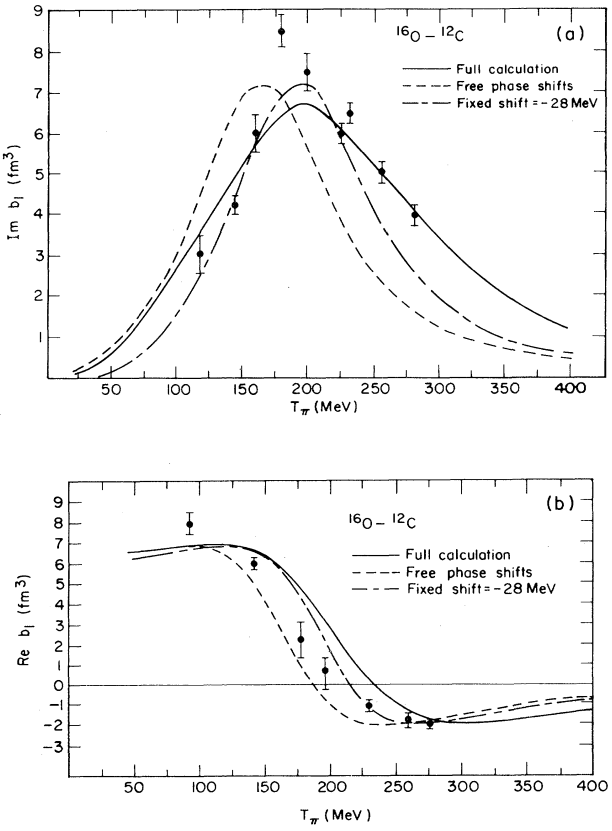

FIG. 3. Effective p-wave strengths for light nuclei as a function of pion energy. Both the imaginary (a) and real (b) parts are given for $l_\pi=0$. The points are taken from Ref. 1.

TABLE I. Rough extraction of the effective modification to the off-shell range as a function of pion kinetic energy. The behavior above 200 MeV does not follow the simple form given by Eq. (37).

T_π (MeV)	$b_1(k_0+1)/b_1(k_0)$	Λ_π (MeV/c)
100	0.95	1470
150	0.71	531
160	0.71	527
170	0.76	618
180	0.86	920
190	0.99	1040

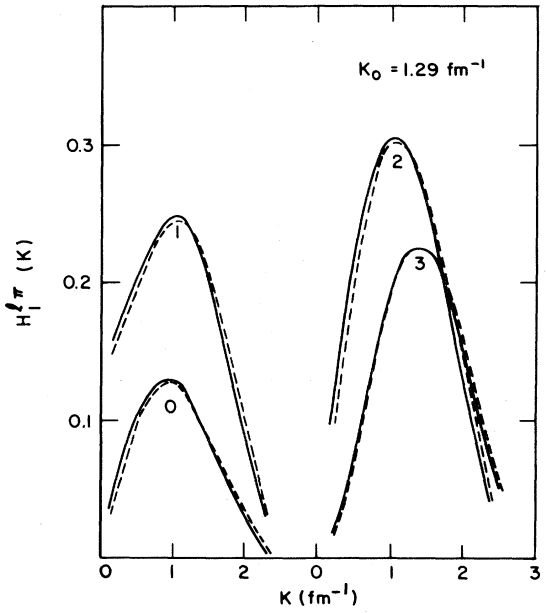

FIG. 4. The off-shell effect in ^{12}C. It is the relationship between the solid $[H(E,k_0,k)]$ and dotted $[\tilde{H}(E,k_0,k)]$ curves that is expressed by Eq. (37) and Table I. The labels give the values of l_π.

The resulting potential was then inserted into a standard optical model code. The value of the off-shell range was not extremely important in the elastic scattering but was important in the charge exchange calculations presented in Sec. V. The calculation of the π^+ elastic scattering on ^{12}C at 162 MeV is shown in Fig. 5. The agreement is considered very good for a *calculation,* not a fit.

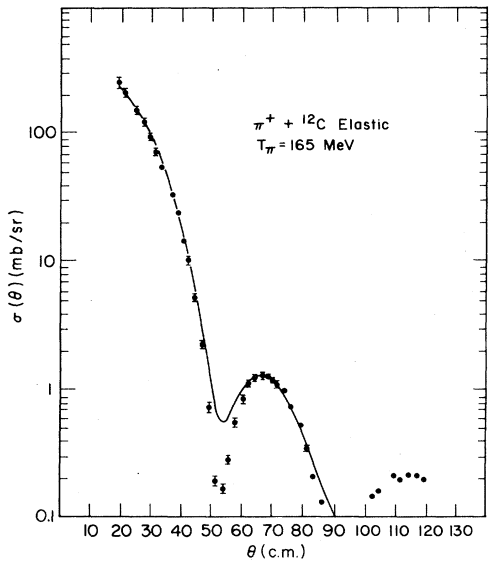

FIG. 5. Elastic scattering from ^{12}C at 165 MeV. The data are from Ref. 1.

IV. VARIATIONS OF THE MODEL

A. Dependence on pion-nucleon potentials

To estimate the effect of replacing t by v in the blocked partial waves we use the finite-range separable model of Thomas.[21] The (real) potential in the (l,I,J) partial wave is given by

$$V_{lIJ}(k,k')=\lambda_{lIJ}g_{lIJ}(k')g_{lIJ}(k)\ , \tag{38}$$

where $g_{lIJ}(k)$ are form factors given by Eqs. (3.13) and (3.14) of Ref. 21. The corresponding t matrix is

$$t_{lIJ}(k',k,E)=v_{lIJ}(k',k)/R_{l,2I,2J}(E)\ , \tag{39}$$

where

$$R_{l,2I,2J}(E)\equiv 1-\lambda_{lIJ}\mathrm{P}\int_0^\infty \frac{dp\,p^2 g_{lIJ}^2(p)}{E-E(p)} + i\pi\mu(k)\lambda_{lIJ}kg_{lIJ}^2(k)\ , \tag{40}$$

and P denotes principal value. Below threshold the imaginary term is not present. $\mu(k)$ is the pion-nucleon reduced energy and $E(p)$ is the center-of-mass kinetic energy of the pion-nucleon system.

For the s waves $|R_{S11}|\cong 0.8$ and $|R_{S31}|\cong 2.6$ in most of the region of interest. The replacement of t by v in blocked levels induces a substantial change in $\mathrm{Re}b_0$. This is especially evident at low energies in the isoscalar amplitudes

$$b^{(+)}=\tfrac{1}{3}(b_{S11}+2b_{S31})\ . \tag{41}$$

The delicate cancellation of the t matrix near threshold (due to chiral symmetry) does not occur for the potentials. This is illustrated clearly in Fig. 6. The b's have been plotted as a function of T_π for peripheral ($l_\pi=kR$) and (for one case) the central ($l_\pi=0$) partial waves. The example is for ^{36}A which is an $N=Z$ nucleus; hence only the isoscalar amplitudes contribute. The steep rise of $\mathrm{Re}b_0$ at low energies was seen in the phenomenological fits of Auerbach *et al.*[22] who also suggested its possible origin. Also shown in the figure are calculations without blocking and with t replaced by zero for the blocked states. It is evident that $\mathrm{Im}b_0$ is suppressed at low energies in accord with empirical studies.[22] The effect is most prominent in the central partial waves.

Figure 6 also displays the strengths for p waves. Since the potentials are real the form of the potential is irrelevant for $\mathrm{Im}b_l$, the results being the same as if t were zero in the filled shells. As with the s waves the suppression of $\mathrm{Im}b_1$ is evident at low energies.

The situation is less clear for $\mathrm{Re}b_1$. In the model of Thomas[21] the large $P33$ wave corresponds to a rather small potential; the large phase shift is due to the smallness of $|R_{P33}|$. The small $P31$ and $P11$ waves both have $|R|\cong 1$ and so also will contribute little. (Actually, as Thomas points out, the $P11$ potential is not to be trusted since the wave is not well fit by a single term separable potential; see Refs. 23 and 24.) For the $P33$, $P31$, and $P11$ waves the replacement of t by zero for blocked levels is a

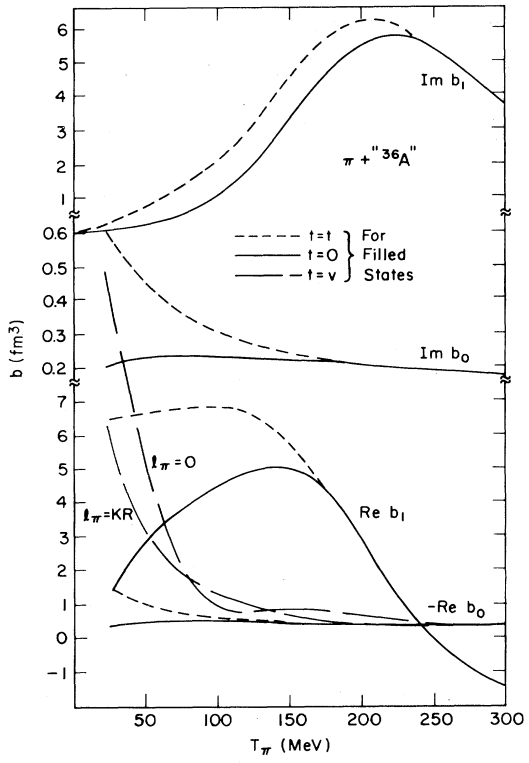

FIG. 6. Blocking effects in "^{36}A." Note that there is a large difference for the s-wave strength with the use of the potential instead of zero.

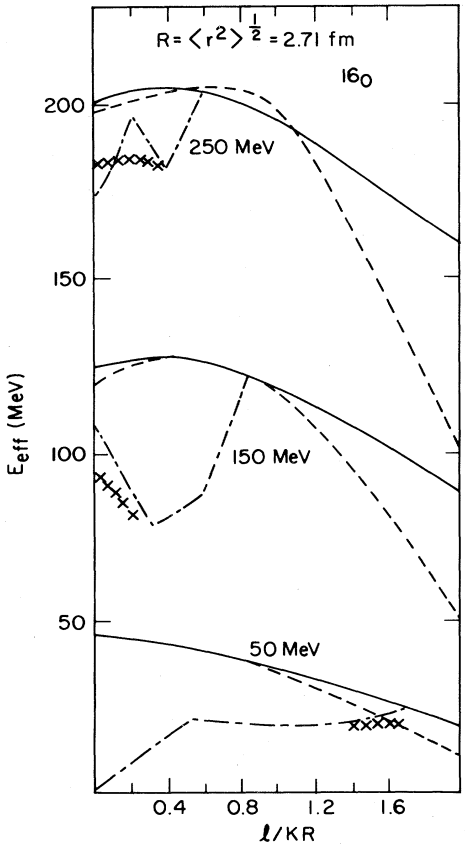

FIG. 7. The effective energy for pion scattering from ^{16}O as defined by Eq. (30). —— represents a calculation with harmonic oscillator potentials (no blocking); $\times\times\times$, harmonic oscillator potentials (blocking); — — — infinite square well (no blocking); and —·—·—·, infinite square well (blocking).

reasonable approximation. The $P13$ wave presents problems, however. It is small and not well determined. The model of Thomas gives $|R_{P13}| \cong 20$ and thus the corresponding potential is very large. This may be an artifact of the model and we have hesitated to apply it in our calculation. Consequently we have used the $t \rightarrow v$ prescription for s waves alone.

To get some indication of the effect of blocking we have as in Sec. III replaced t_1 by zero for the blocked levels. Actually, the phenomenological results of Ref. 22 for Reb_1 are rather closer to the unblocked results. A fuller study of the "small" p-wave amplitudes with an eye to evaluating the effective potentials would clearly be worthwhile.

B. Isovector nuclei

When dealing with nuclei having $N \neq Z$ we rewrite Eq. (25) as

$$\langle \vec{k}' | V^{\pm}_{\rm opt}(E) | \vec{k} \rangle = \sum_{L\alpha\alpha'} [N_\alpha \theta^{\alpha\alpha'}_{L\pi^\pm{\rm n}}(k,k') + Z_\alpha \theta^{\alpha\alpha'}_{L\pi^\pm{\rm p}}(k,k')] H^{l_\pi}_{\alpha\alpha' L}(k,k') P_{l_\pi}(x) ,$$

where $(2l+1)Z_\alpha$ and $(2l+1)N_\alpha$ are the numbers of neutrons and protons in the α shell. We have taken the neutron- and proton-core potentials the same except for a possible additive constant. A constant added to the potential will have no effect upon $\theta^{\alpha\alpha'}$ as it is a function of the difference $E_\alpha - E_{\alpha'}$.

C. Harmonic oscillator nucleus

The square well model we have used in the previous calculations is not particularly realistic. To assess the model dependence in our average b's due to the choice of radial wave functions we have recomputed some of our results using oscillator states. We have, for comparison, picked examples in which the same shells were assumed filled. The spin-orbit potential is absent in both models and hence the shell closings do not occur at the proper magic numbers. In future work we expect to use more realistic nuclear models, but for a study of the general trends with nuclear size our models should be adequate.

The dependence of the effective energy [Eq. (30)] upon the choice of radial wave functions is shown in Figs. 7 and

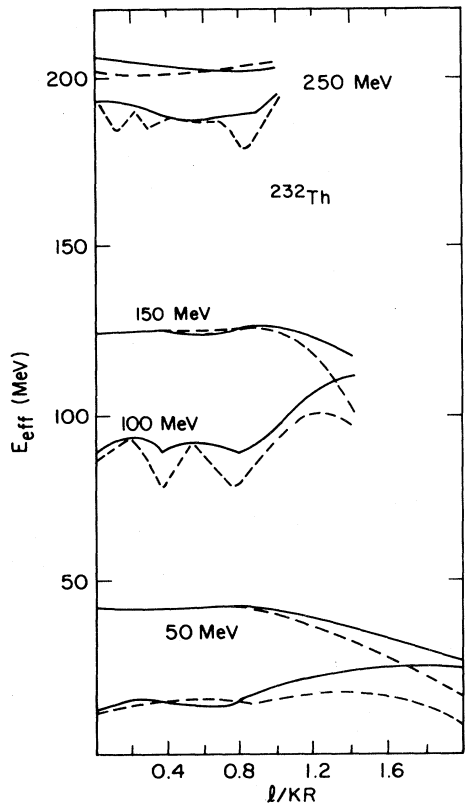

FIG. 8. The effective energy for pion scattering from "^{222}Th." See Fig. 7 for an explanation of the curves.

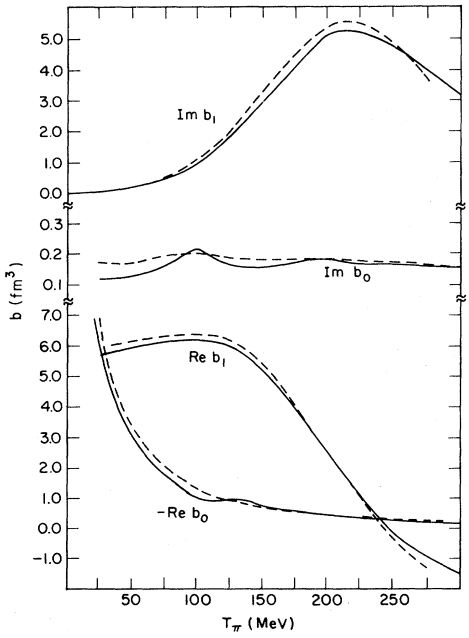

FIG. 9. Effective strengths for the scattering of pions from "^{222}Th," central partial waves. The dotted curve is for a harmonic oscillator potential and the solid curve is for an infinite square well.

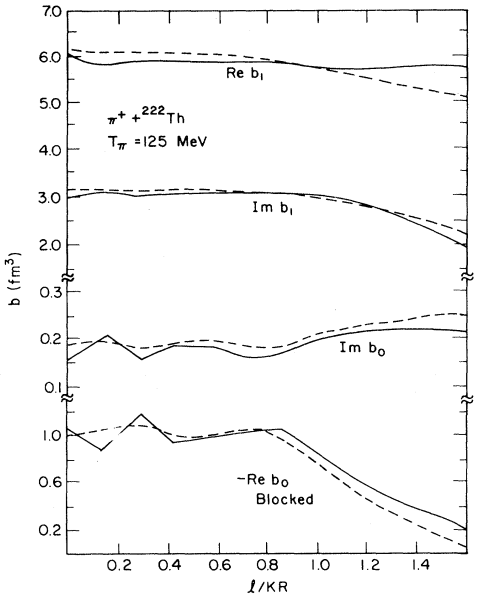

FIG. 10. Dependence of the effective strengths of the pion partial wave.

8. The curves for a heavy nucleus (Th) are flatter for small l_π but otherwise quite comparable with those of a light nucleus (^{16}O). The oscillator and square well effective energies differ widely for very large l_π/kR; however, these peripheral waves contribute less to the cross section. Also shown is the effect of Pauli blocking upon energy shifts; terms in Eq. (30) are omitted if the intermediate level is filled. Since the blocking affects only the partial waves $l_\pi \leq 2l_{\max}+1$, where $l_{\max}$ is the highest l present in the nuclear wave function, the effect is most prominent for large nuclei at low energies. At energies below 150 MeV and for the lower partial waves the effective shift due to the Pauli exclusion is comparable to the binding. This "Pauli shift" becomes smaller at higher energies. (This prescription makes more sense for Imb since Im$\theta=0$ for blocked levels.) It is also of note that at $T_\pi \leq 150$ MeV the Pauli shift affects only impact parameters of less than the nuclear radius and hence would not be important for extreme surface peaked reactions.

The strengths corresponding to the previous energy shifts are given in Figs. 9 and 10. Figure 9 gives the b's as a function of energy for the central partial wave and Fig. 10 gives the b's as a function of l_π at 125 MeV. These results confirm the rather weak dependence of the effective b's on the single particle potential except at large impact parameters.

D. Isotope effects

The final set of figures in this section compares the b's corresponding to the pair of isotopes, ^{222}Th and ^{228}Th. Figure 11 shows a comparison of the strengths of the central partial wave ($l_\pi=0$) as a function of energy. As may be seen, the effect is not large. All curves were calculated with single particle wave functions taken from the infinite square well. The strengths at 125 MeV for various partial

waves are plotted in Fig. 12. Note that the effect displayed is the minimal one expected (barring cancellations from other sources). The changes in radius due to the increasing number of nucleons and true pion absorption will also affect these differences.

This section has presented some examples of quantities which can be computed with this type of model. Clearly, considerable improvements are needed (primarily in the single particle model, the pion-nucleon potential, and the addition of true absorption).

V. PION CHARGE EXCHANGE

In this section we present the results of the calculations of analog charge exchange in three nuclei. The calculations are done in distorted wave impulse approximation with the transition t matrix given by

$$t_t=\lambda_0(E)+\lambda_1(E)\vec{q}\cdot\vec{q}\,' .$$

Here we have neglected spin flip (about 10% in the ^{13}C total cross section but a substantial error in the ^{7}Li case). The quantities $\vec{q}$ and $\vec{q}\,'$ are treated as gradient operators on the initial (π^+) and final (π^0) wave functions. The parameters λ_0 and λ_1 are calculated from the charge exchange amplitude obtained from the phase shifts. Two possibilities are considered: The phase shifts are evaluated at (1) the incident energy or (2) the shifted (but not blocked) phase shifts from Sec. III are used. We are not presenting a theory of this t matrix but investigating the effect of medium corrections on distorting waves used in the calculation of the charge-exchange cross sections. An extension of Sec. IV B may provide such a theory in the future, but since the present paper deals only with closed shells (clearly we already make an approximation to apply our results to most nuclei), charge exchange on an odd particle is not included in our medium corrections.

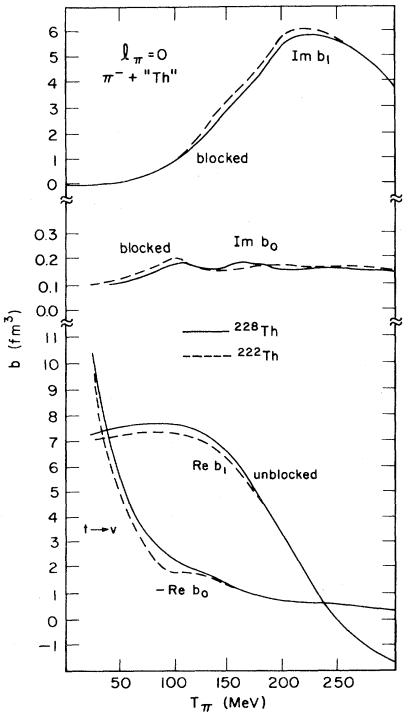

FIG. 11. The effect of different shell closures for $l_\pi=0$. The strengths for ^{222}Th (dotted) have the last shell $1h$ and the ones for ^{228}Th have an additional $3P$ shell filled.

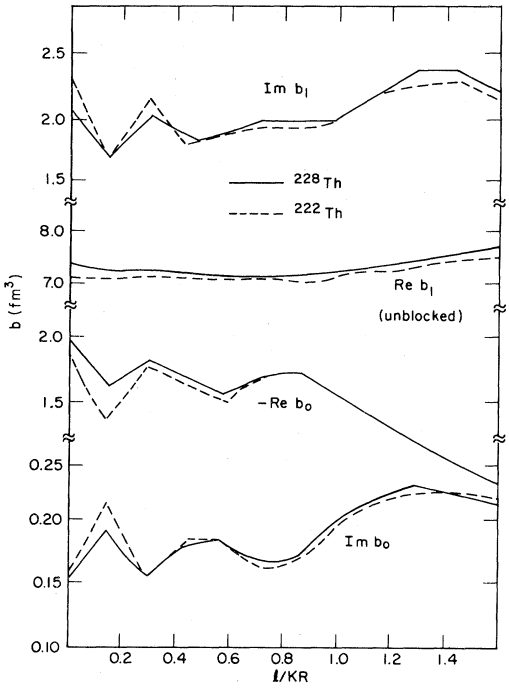

FIG. 12. The effect of shell closure as a function of the pion-nucleus partial wave at $T_\pi=125$ MeV.

Since our present model is restricted to closed shell nuclei the distorted waves are calculated with ^{16}O shell structure, but with a body density scaled to the appropriate nucleus. The blocking effect is probably fairly estimated for ^{15}N and ^{13}C but may be poorly estimated for ^{7}Li. The transition densities are obtained from the product of wave functions which are solutions in a Saxon-Woods well with the proper binding energy (and Coulomb potential in the final state). The overlap of these two functions is nearly unity. Data used for comparison in this section were taken at the π^0 spectrometer at the Los Alamos Meson Physics Facility (LAMPF). The cross sections can be found in Refs. 25 and 26. More details are available in the thesis of Doron.[27]

Figure 13 shows the 0° cross section for the analog charge exchange cross section on ^{13}C. The two dashed curves use free phase shifts for the transition t matrix. The short dashed curve has no blocking while the long dashed curve has blocking. The solid curve uses the transition t matrix computed with energy shifted phases and blocking in the distorted wave. Note that the blocking effects diminish above 240 MeV, being largest around 120—140 MeV. The energy shift effects are small at low energy. A substantial increase in the calculated cross section is obtained from the blocking of the distorting waves.

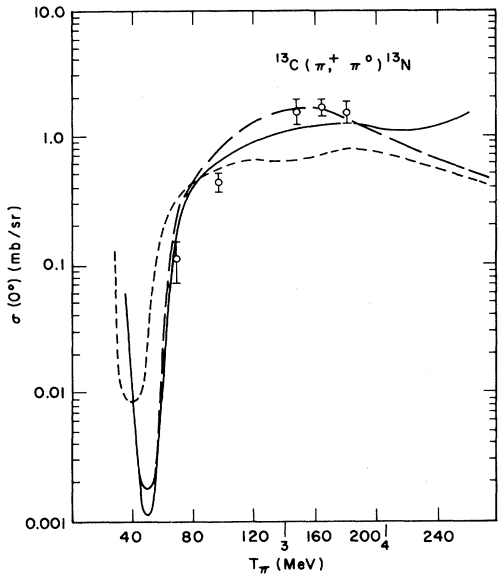

FIG. 13. Zero degree analog cross section on ^{13}C. The two dashed curves use free phase shifts in the transition t matrix, while the solid one uses energy-shifted phase shifts. The long dashed and solid curves include Pauli blocking effects in the distorted waves. The small "3" and "4" mark the position of $qR=3$ and 4.

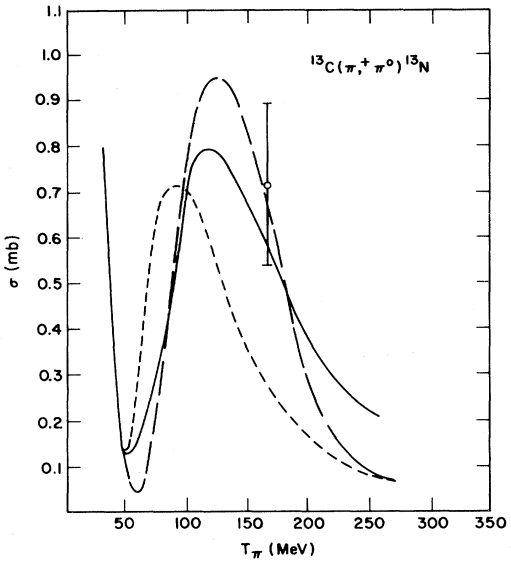

FIG. 15. Integrated cross section for pion charge exchange on ^{13}C as a function of incident pion energy. See the caption of Fig. 13 for the meaning of the curves.

Note that when a certain set of waves is blocked (here we are considering $1s$ and $1p$ waves) the π-nucleus waves affected must be $\leq 2l_{\max}+1$ [see Eq. (26) with $l=l'=1$ and $L=1$ for the case in question here]. When this wave is at the surface of the nucleus we may expect the maximum effect. For the carbon case this point in energy is marked with the small "3." If a (more realistic) spin-orbit model were used one would expect the condition to be $\leq 2j_{\max}+1$, which for carbon gives 4. The point for $kR=4$ is marked with the small "4." Thus we may anticipate that the introduction of a spin-orbit force would probably push the blocking effects to slightly higher energies.

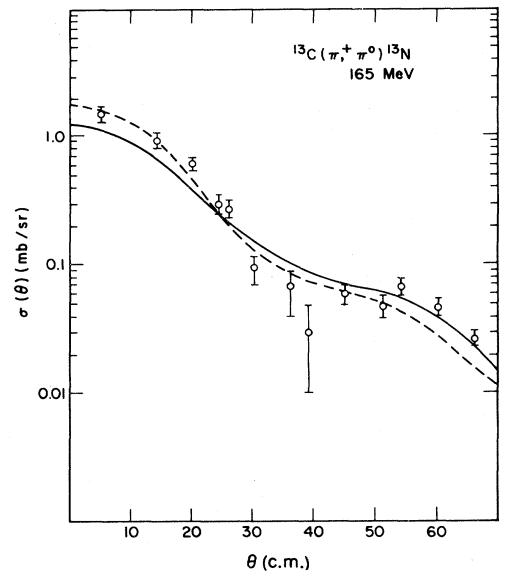

FIG. 14. Angular distribution of pion charge exchange on ^{13}C at 165 MeV. Both curves include Pauli blocking effects in the distorted waves. The dashed curve uses free phase shifts in the transition t matrix.

Figure 14 shows the comparison with the ^{13}C angular distribution at 165 MeV. The agreement with the forward angles is very good for the free (transition t matrix) phase shift case. There are several possible reasons for the lack of agreement at back angles. First, the spin-flip charge exchange (left out of this calculation) is largest there, and second, the measurement is actually of the ground plus first excited state. The major contribution of the first excited state is expected to be at larger angles.

Figure 15 shows the total cross section for ^{13}C. The same remarks about the spin flip and the first excited state apply here as well. The presence of the strong dip around 60 MeV is notable.

In Fig. 16 the 0° cross section of charge exchange on ^{15}N is shown. The solid curve uses energy shifted transition t-matrix phase shifts and blocked distorted waves while the dashed curve has no blocking. The deep minimum is in agreement with data. Figure 17 shows the corresponding total cross section with the same convention for the curves. Figure 18 compares the calculation with the two measured angular distributions. The agreement is generally good with the exception of the second maximum. It is possible that the neglected spin flip is playing a role here as well.

For completeness we show (Fig. 19) the 0° charge exchange on ^{7}Li. This nucleus is far from a closed shell so the model is least applicable. The spin flip effect is known to be large in this nucleus so the total cross sections are expected to be in error (and are).

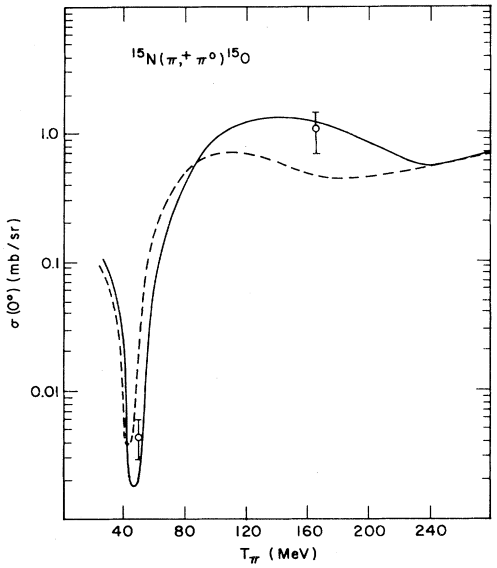

FIG. 16. Zero degree analog cross section for pion charge exchange on ^{15}N. The solid curve has Pauli blocking effects included in the distorted waves. Both are calculated using energy-shifted phase shifts in the transition t matrix.

VI. CONCLUSIONS AND QUESTIONS

We have shown that corrections due to the nuclear medium on the distorted waves used to calculate pion charge exchange are significant. Moreover, the corrections improve the agreement between experiment and theory appreciably. A number of open questions remain, however.

What is the effect of the neglect of recoil? This is known to be important in elastic scattering at low energies

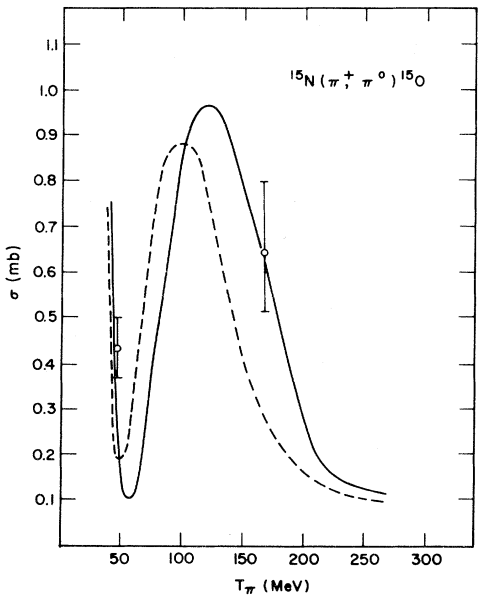

FIG. 17. Integrated cross section for pion charge exchange on ^{15}N as a function of incident pion energy. See Fig. 16 for an explanation of the curves.

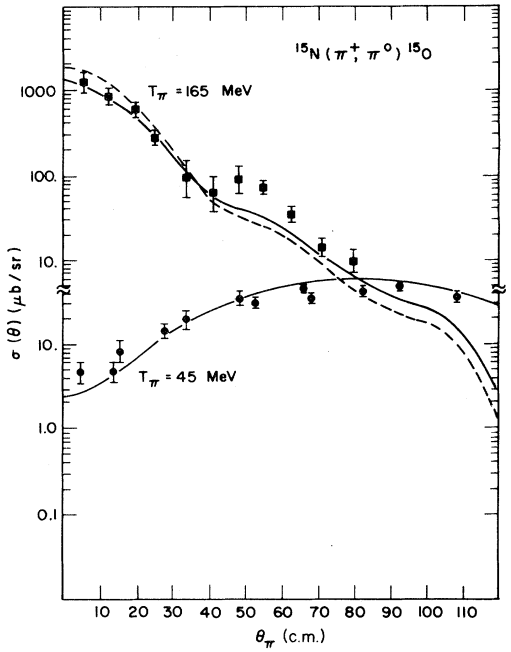

FIG. 18. Angular distribution of pion charge exchange on ^{15}N at 48 MeV (lower curve) and 165 MeV (upper curve). The solid curve uses a free charge exchange transition t matrix while the long dashed curve is due to a shifted t matrix. Pauli blocking effects are included in all curves.

but the effect on the distorted waves is unknown. We are currently studying methods for including this correction.

Are the approximations made in reducing to the standard form of the off-shell dependence of the optical model reasonable? These can be checked by solving the full mul-

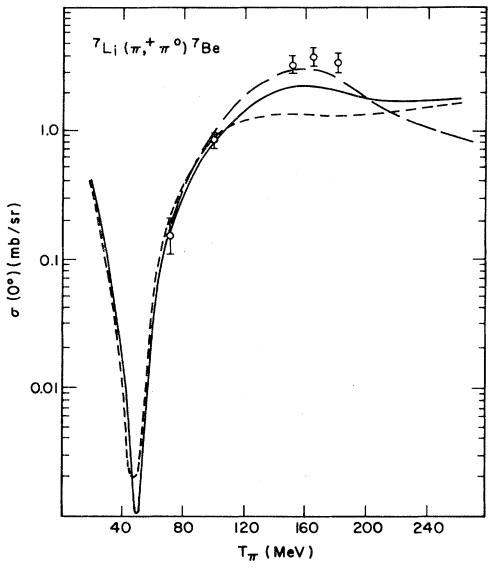

FIG. 19. Zero degree cross section for pion analog charge exchange on ^{7}Li. The short dashed curve is calculated with shifted distorted waves and transition t matrix but no blocking. The other two curves have blocking but one (solid) has a shifted transition t matrix while the other (long dashed) has a free transition t matrix.

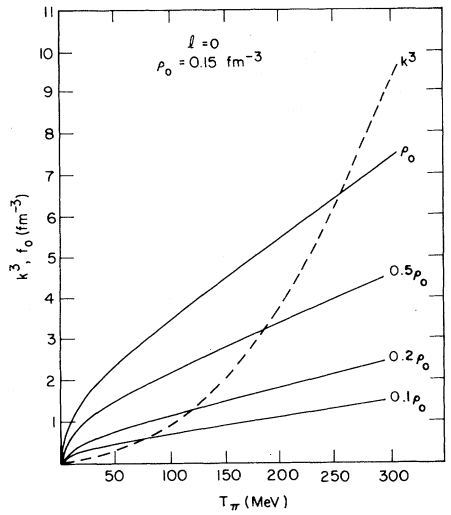

FIG. 20. Comparison of f_0 [as defined by (A3)] with k^3.

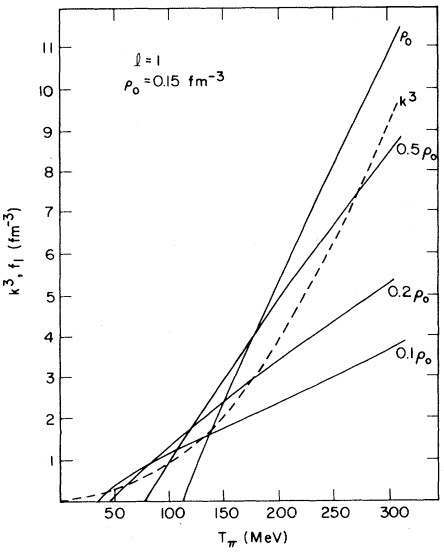

FIG. 21. Comparison of f_1 [as defined by (A3)] with k^3.

titerm potential. The possibilities for doing this are also under study.

What is the role of true absorption? This question is difficult, especially when dealing with the surface peaked reactions treated here. If annihilation takes place on two nucleons it will occur slightly inside the surface region (since its absorption potential follows a roughly ρ^2 dependence) and the effect on the reaction will be moderate. If, in fact, the average absorption takes place on several nucleons the effect will be much smaller since the absorption will be more localized to the center of the nucleus and hence away from the reaction region.

What is the effect of the spin-orbit potential in the intermediate well? From the arguments given in Sec. V for ^{13}C we might expect moderate changes in Pauli blocking effects.

What is the effect of the confining well assumed in the present work? It may be expected that the approximation used in this work is reasonable with the exception of the effect of the Coulomb potential on the ejected nucleon. This last effect is potentially crucial for π^+-π^- comparisons and measurements of neutron radii. A solution to this more difficult problem is being considered but may require considerably more computation than the model considered in this paper.

Two recent works which treat Pauli blocking effects in a spirit similar to that of the present work (but do not compute the effect on charge exchange) are those of de Kam[28] and Seki *et al.*[29]

ACKNOWLEDGMENTS

One of us (W.R.G.) would like to acknowledge valuable conversations with H. Garcilazo, N. Austern, J.-P. Dedonder, and B. F. Gibson. We would like to thank the π^0-spectrometer group at LAMPF for allowing us to see their data before publication. This work was supported by the United States Department of Energy.

APPENDIX: SEMICLASSICAL DISCUSSION

It has been suspected for several years that the pion nucleus optical model is too absorptive in the region of the 3-3 resonance. This is apparent when one considers the fact that the simple t-ρ prescription is approximately equivalent to the usual mean-free-path argument that gives that $\lambda = 1/\sigma\rho$, where σ is the cross section and ρ is the (in this case, nuclear) density. Plots of λ versus energy are common and many people have noticed that, near the resonance, the mean free path becomes less than 1 F, which is smaller than the internuclear distance (around 1.5 F). This seems unlikely to happen in the physical world since classically it is impossible to strike the next particle until it is encountered, no matter how large the cross section. This naive expectation may be wrong for two reasons. The first is that we are dealing with extended interaction regions. Thus it is possible to encounter two (or many) particles at once. In this manner it is possible to have continuous interactions and thus a zero mean free path. The second reason is that we are dealing with a quantum mechanical system.

It is useful to state the intuitive condition in terms of the quantum language. We assume that the interaction takes place in a single partial wave l. Thus we use an estimate of the size of the interaction region as l/k so that the condition (for spheres of radius l/k) becomes

$$1/\rho\sigma < 1/\rho^{1/3} - 2l/k \tag{A1}$$

or

$$l < \sigma\rho^{2/3} - 2l\sigma\rho/k \ . \tag{A2}$$

Note that the maximum cross section in a single partial wave is

$$4\pi(2l+1)/k^2$$

so that the condition

$$k^3 < (2l+1)4\pi\rho^{2/3}k - 8\pi l\rho(2l+1) \equiv f_l \qquad \text{(A3)}$$

results. For $l \neq 0$ the second term is zero so the solution to the limiting equation is trivial, giving $k = 321$ MeV/c for $\rho = 0.15$ fm^{-3}. Thus we see that for zero size ($l = 0$) objects our intuitive classical limit has the quantum analog that the incident momentum must be greater than the Fermi momentum in the nucleus. We plot the comparisons of k^3 vs f_0 and f_1 in Figs. 20 and 21. One must determine in what region of the nucleus the transition density peaks in order to know the effect of the blocking on any particular reaction. If the pionic wave function in the center of the nucleus is needed, the blocking effects extend to high energies. However, few reactions sample this region so this may not be very relevant. More commonly, transition densities and absorption effects (which will still remain moderately large) limit the reaction to the region between $\frac{1}{2}$ and $\frac{1}{10}$ of the central density. Thus one may expect enhancements (of greater or lesser amounts depending on the details of the transition density) in the region of the lower half of the 3-3 resonance (80—170 MeV). This is the semiclassical picture which underlies the full quantum treatment given in the text.

[1]W. B. Cottingame and D. B. Holtkamp, Phys. Rev. Lett. 45, 1828 (1980).

[2]C. Schmit, Nucl. Phys. A197, 449 (1972).

[3]J. Revai, Nucl. Phys. A205, 20 (1973).

[4]C. Schmit, J. P. Dedonder, and J. P. Maillet, Nucl. Phys. A239, 445 (1975).

[5]J. M. Maillet, J. P. Dedonder, and C. Schmit, Nucl. Phys. A271, 253 (1976).

[6]P. C. Tandy, E. F. Redish, and D. B. Bollé, Phys. Rev. Lett. 35, 921 (1975); Phys. Rev. C 16, 1924 (1977).

[7]L. C. Liu and C. M. Shakin, Phys. Rev. C 16, 333 (1977).

[8]R. H. Landau and A. W. Thomas, Nucl. Phys. A302, 46 (1978).

[9]J. Maillet, J. P. Dedonder, and C. Schmit, Nucl. Phys. A316, 267 (1979).

[10]M. Silver and N. Austern, Phys. Rev. C 21, 272 (1980).

[11]H. Garcilazo and W. R. Gibbs, Nucl. Phys. A356, 284 (1981).

[12]R. H. Landau and M. McMillan, Phys. Rev. C 8, 2094 (1973).

[13]R. H. Landau and A. W. Thomas, Phys. Lett. 88B, 226 (1979).

[14]W. R. Gibbs, B. F. Gibson, A. T. Hess, G. J. Stephenson, Jr., and W. B. Kaufmann, Phys. Rev. Lett. 36, 85 (1976).

[15]W. R. Gibbs, in *Theoretical Methods in Medium-Energy and Heavy Ion Physics,* edited by K. W. McVoy and W. A. Friedman (Plenum, New York, 1978), pp. 503—531.

[16]J. M. Eisenberg, J. Hufner, and E. J. Moniz, Phys. Lett. 47B, 381 (1973).

[17]H. Garcilazo and W. R. Gibbs, Nucl. Phys. A381, 487 (1982).

[18]W. R. Gibbs, B. F. Gibson, and G. J. Stephenson, Jr., Phys. Rev. Lett. 39, 1316 (1977).

[19]L. S. Kisslinger and W. L. Wang, Phys. Rev. Lett. 30, 1071 (1973); Ann. Phys. (N.Y.) 99, 374 (1976); M. Hirata, F. Lenz, and W. K. Yazaki, *ibid.* 108, 116 (1977); M. Hirata, J. H. Koch, F. Lenz, and E. J. Moniz, *ibid.* 120, 205 (1979); K. Klingenbeck, M. Dillig, and M. G. Huber, Phys. Rev. Lett. 41, 387 (1978); E. Oset and W. Weise, Nucl. Phys. A329, 365 (1979); J. H. Koch and E. J. Moniz, Phys. Rev. C 20, 235 (1979).

[20]A. N. Saharia, R. M. Woloshyn, and L. S. Kisslinger, Phys. Rev. C 23, 2140 (1981).

[21]A. H. Thomas, Nucl. Phys. A258, 417 (1976).

[22]E. H. Auerbach, D. M. Fleming, and M. M. Sternheim, Phys. Rev. 162, 1683 (1967).

[23]B. Blankleider and I. R. Afnan, Phys. Rev. C 24, 1572 (1981).

[24]A. S. Rinat *et al.*, Nucl. Phys. A329, 285 (1979).

[25]H. W. Baer *et al.*, Phys. Rev. Lett. 45, 982 (1980).

[26]A. Doron *et al.*, Phys. Rev. C 26, 189 (1982).

[27]A. Doron, Ph.D. thesis, Tel-Aviv University, 1981.

[28]J. de Kam, Phys. Rev. C 24, 1554 (1981).

[29]R. Seki, K. Masutani, and K. Yazaki, Phys. Rev. C 27, 2817 (1983).